

DETECTION OF STRUCTURED LASER BEAM CENTROID AND ITS USE FOR ALIGNMENT

Martin DUSEK, CERN, Geneva Switzerland, and TUL, Liberec, Czech Republic
Krystof POLAK, CERN, Geneva, Switzerland and TUL, Liberec, Czech Republic
Jean-Christophe GAYDE, CERN, Geneva, Switzerland
Miroslav SULC, TUL, Liberec, Czech Republic
Dirk MERGELKUH, CERN, Geneva, Switzerland
Witold NIEWIEM, CERN, Geneva, Switzerland and ETH, Zurich, Switzerland

Abstract

A Structured Laser Beam (SLB) [1] is a pseudo-non-diffractive optical beam. Its transverse profile is similar to a Bessel Beam (BB), hence its bright central core is surrounded by concentric circles. SLB can propagate with very low divergence over long distances. Propagation over 200 m has been tested with a divergence under 0.01 mrad. Therefore, the central core can still fit on the camera chip and its centroid position can be accurately detected, which is not the case for well-known Gaussian beams (GB). These properties make the SLB a promising candidate for long-distance alignment applications because it could be used as a reference line.

The alignment accuracy is affected by the algorithms for centroid detection. In this work, different algorithms for centroid position detection are evaluated and compared on simulated data, namely the best fitting of a well-parameterized Bessel function and different alternations of the center of gravity methods. In addition to simulations, real data are obtained during experiments using a high-precision motorized stage to induce a known translation of a sensor resulting in misalignment. This misalignment is compared with the misalignment detected by an SLB sensor. Therefore, the potential of SLB for long-distance alignment is explored.

INTRODUCTION

The alignment of accelerator components with high accuracy is a challenging task. At CERN straight-line reference systems have been developed to meet the tight accuracy needs. The principle of the systems is based on stretched wires (Wire Positioning System) and water level (Hydrostatic Leveling System) [2]. These systems are precise in the order of micrometers over hundreds of meters, however, have drawbacks such as cost or implementation difficulties. It is also difficult to find a system that could give similar results for the comparison. Hence using a laser as a reference line can be a viable alternative.

The laser light path is assumed to be a straight line. Note that this has to be investigated due to refraction and symmetry breaking [3]. Systems with laser beams propagating in a vacuum, to minimize the effect of refraction caused by air fluctuations, have been developed for several accelerators. Japanese High Energy Accelerator Research Organization (KEK) uses mechanically switched quadrant-

photodetectors to detect the laser propagating inside a vacuum tube [4]. Estimated accuracy is 100 μm over 500 m. The quadrant-photodetectors however have a drawback, if there is an irregularity in the laser spot shape, the centroid detection accuracy can be strongly affected.

The Compact Linear Collider (CLIC) [5] is a proposed accelerator that is under study at CERN. The project has quite tight alignment tolerances of 10 μm over 200 m. The LAMBDA sensor was in development for this task [6]. The principle lies in projecting a GB propagating through a vacuum on a plate. The plate is movable, therefore it can block the path of the laser when moved in. The projection of the GB is then viewed with the camera and the center is calculated and measured using Gaussian function fitting and photogrammetry. However, this system has several disadvantages. After propagation of 200 m, most of the intensity is lost and the ability for precise detection of the center is affected due to the divergence and beam energy loss. The other source of error is the photogrammetric camera objective, which induces field deformation due to lens aberrations, and also brings additional calculation steps.

The Structured Laser Beam has the potential for long-distance alignment due to its extremely low divergence and sharply defined core, which can fit on a reasonably sized chip even after propagating for 120 m (figure 5). This allows us to read the image straight from the camera chip, without using any optics, and use highly precise algorithms for center detection. This can potentially eliminate the drawbacks of the LAMBDA sensor and quadrant-photodetector systems.

To meet the tight alignment tolerances, algorithms for centroid detection with sub-pixel accuracy need to be implemented. The centroid detection will be discussed in the following chapters together with the investigation of the refractive index fluctuation effect of the medium of propagation. The resulting data should highlight the potential of SLB for long-distance alignment applications.

DETECTION OF A BEAM CENTROID

Center of Gravity

The Center of gravity (CoG) algorithm, the so-called first moment weighted by intensity, is widely used in different image processing applications [7]. It is not computationally expensive and reaches sub-pixel accuracy. The centroid coordinates \bar{x} and \bar{y} are calculated as:

$$\bar{x} = \frac{\sum_{x=0}^{x_{max}} \sum_{y=0}^{y_{max}} I(x, y)x}{\sum_{x=0}^{x_{max}} \sum_{y=0}^{y_{max}} I(x, y)} \quad (1)$$

$$\bar{y} = \frac{\sum_{x=0}^{x_{max}} \sum_{y=0}^{y_{max}} I(x, y)y}{\sum_{x=0}^{x_{max}} \sum_{y=0}^{y_{max}} I(x, y)} \quad (2)$$

where $I(x, y)$ is the measured intensity at a given pixel row x and column y of an image.

The preprocessing of an image can reduce noise in the image and increase the accuracy of CoG algorithms. In our case thresholding and gamma correction were used and will be referred to as the TCoG and GCoG respectively.

The TCoG algorithm uses the thresholding function $T(x, y)$ which sets the pixel value to zero when its intensity is lower than the threshold level t after background subtraction:

$$T(x, y) = \begin{cases} I(x, y), & I(x, y) \geq t \\ 0, & I(x, y) < t \end{cases} \quad (3)$$

In the case of GCoG, we introduce a non-linear relationship between pixel intensity levels using function G_{corr} . Hence low-intensity values are lowered and high-intensity values are enhanced:

$$G_{corr}(x, y) = I_{max} \left(\frac{I(x, y)}{I_{max}} \right)^\gamma \quad (4)$$

As the value of gamma parameter γ increases, the upward-sloping of the function is larger, hence the bigger the relative difference between the intensity levels.

Best fitting of a well-parameterized Bessel function

Best-fit algorithm (BFA) finds the optimal parameters of the equation describing the BB intensity distribution, to match the shape of the observed beam. The intensity distribution of a BB with the center intensity normalized to one is described as:

$$I(x, y, \bar{x}, \bar{y}, k_T) = \left(J_0 \left(k_T \sqrt{(x - \bar{x})^2 + (y - \bar{y})^2} \right) \right)^2 \quad (5)$$

where J_0 is a Bessel function of the first kind and zero order, k_T is the transverse wave vector. The parameters k_T , \bar{x} and \bar{y} are the subject of change during the optimization process which roughly estimates the values. After the optimization, the precise positions of \bar{x} and \bar{y} are found using non-linear least-squares fitting:

$$\underset{\bar{x}, \bar{y}}{\text{minimize}} I(x, y, \bar{x}, \bar{y}, k_T) = \sum_{i=0}^m I(x, y, \bar{x}, \bar{y}, k_T)^2 \quad (6)$$

It is possible to use BFA for the centroid detection of SLB, due to the similarity of the intensity distributions between BB and SLB. Note, that this fact can also be a cause of the error.

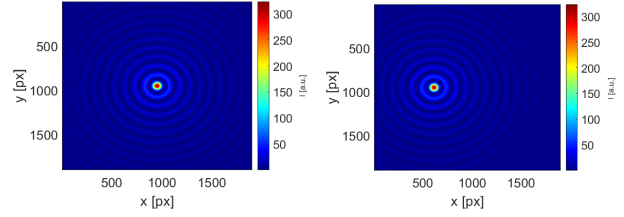


Figure 1: Image of the region of interest (ROI) with the BB centered in the middle of it. Latter image with the BB centroid shifted on X-axis by 320 pixels.

Bessel Beam centroid detection

To investigate the error in centroid detection caused by the fact that the equation 5 does not precisely describe the intensity distribution of an SLB, we used BFA to detect the centroid of a BB first. To be sure that the center of the BB centroid is in a known spot, simulated beam intensity distributions were generated using the software VirtualLab Fusion©. We simulated a system with an NBK-7 glass axicon with an angle of 1° . The size of the output images was 1901x1901 pixels (px).

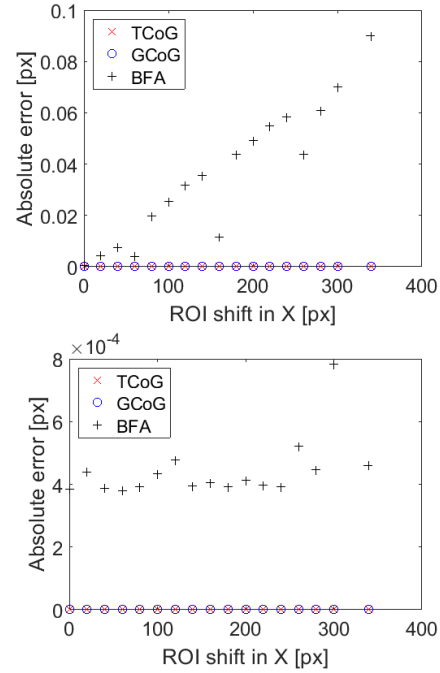


Figure 2: Absolute error of BB centroid coordinates dependency on ROI shift in X-direction for \bar{x} (top) and \bar{y} (bottom).

It was assumed that BFA will be more precise than the algorithms using the CoG principle. To investigate the performance, the rectangular ROI sized 950x950 pixels was extruded out of the original image. The centroids of the ROI and BB were in the corresponding known positions. Later, we introduced a shift of the ROI in the X-axis to have the beam centroid in a different position relative to

the ROI centroid as illustrated in the right part of figure 1.

All of the centroid algorithms with fixed parameters k_T , t , and γ were used to find the centroid in images with linearly increasing shift in the X-coordinate of the ROI. Then we compared the known position of the BB centroid with the one detected. By an absolute error, we mean residual between the known centroid of the beam and the detected one.

The results in figure 2 show that when we introduce a shift in X-axis, the absolute error of the \bar{x} for the BFA is linearly increasing with the shift. While the Y-axis shift remains zero, hence the beam is centered in that axis, the error of \bar{y} does not show the linear trend. CoG algorithms are not affected by the shift in the X-axis, the error remains in the order of 10^{-6} of a pixel and does not show any trend. The process was tested by introducing a shift in Y-axis while X-axis staying the same with a similar result. Hence only the error of \bar{y} was linearly increased with the shift in Y-axis, while the error of \bar{x} remained unaffected.

Structured Laser Beam centroid detection

The algorithms were tested on simulated SLB data as well. The shifting of the ROI in the X-direction was repeated. We can see the same linear trend of the absolute error for BFA which goes up to 0.18 pixels. We believed that this is caused by the fact that some parts of the beam's outer rings are cut out of the image (figure 1). Therefore, the circular mask was used to make sure that only full rings remain in the image (figure 3).

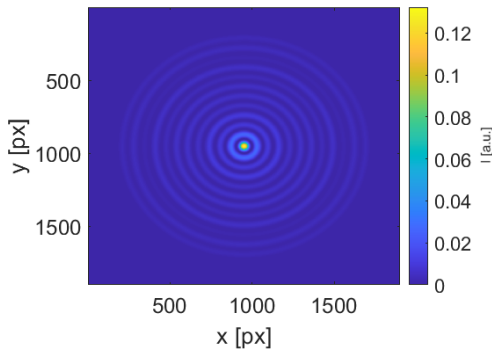


Figure 3: SLB intersected using a circular mask, hence only full beam rings are present in the image.

The results in figure 4 show that masking out the non-full rings significantly lowers the error of BFA and it is no longer linearly dependent on the ROI shift in the X-direction. The error of the GCoG is in the order of 10^{-3} pixels, while the error of the TCoG is in the order of 10^{-5} pixels. After using a mask, the error of BFA is in the order of 10^{-2} pixels.

The CoG algorithms are slightly more accurate and less computationally expensive than BFA. Hence they are suitable for applications where the detection of centroid in multiple images per second is needed (table 1). The TCoG algorithm behaves better for simulated data. However, in

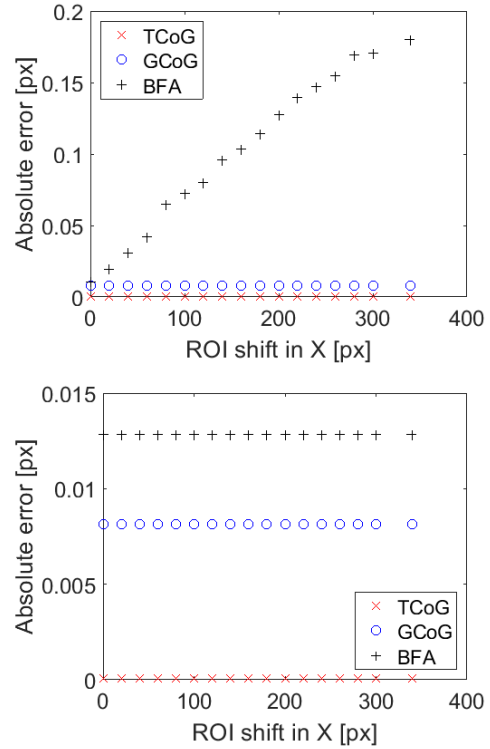


Figure 4: Absolute error of SLB \bar{x} centroid coordinate dependency on ROI shift in X-direction for unmasked (top) and masked (bottom) images respectively.

real conditions, background subtraction has to be done, hence it can be prone to background illumination changes. The algorithm is also sensitive to the changes of threshold level t .

Table 1: Relative computational time for analysis of 1901x1901 pixel image. Implemented in MATLAB.

Algorithm	Computational time
BFA	40.03 s
GCoG	0.17 s
TCoG	0.16 s

The camera chips have a rectangular shape hence the error of the BFA can be significant and depends on the relative position of the beam centroid to the image center. In our simulations, the error was reaching up to 0.18 pixels. The preliminary tests on simulated images with introduced noise show that the absolute error of the BFA caused by the relative beam position can be even higher. This can have a significant effect on high-precision alignment applications. To get rid of this source of error, it is necessary to use a circular mask that cuts out non-full outer beam rings. This is not the case for the CoG algorithms, because the threshold and gamma correction minimizes the influence of the rings on the centroid detection.

LONG DISTANCE ALIGNMENT INVESTIGATION

In this chapter, the potential of the SLB for use in high-precision alignment was investigated also experimentally. Refractive index fluctuations of the propagation media play a major role in laser light alignment systems. The SLB is a novel type of laser beam hence the influence of the phenomenon has not been yet described thoroughly. The SLB propagation and stability were measured over 120 m in one of the CERN underground tunnels (figure 5).

We used the GCoG to detect the centroid with 3 frames per second for 1 hour. Even though the TCoG behaves better on simulated data, in real conditions it is prone to the choice of the optimal threshold level t and background illumination. These effects need to be investigated more to be able to use the TCoG algorithm proficiently. The absolute of the GCoG is not as significant even if the γ is not chosen optimally and the background illumination does not play such a big effect, due to the working principle of the algorithm.

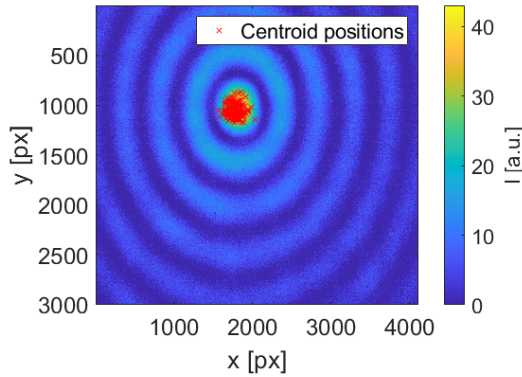


Figure 5: Real image of SLB propagated over 120 m in CERN underground tunnel. Projected on a camera with a chip size of 14.1x10.3 mm and pixel size of 3.45 μm .

The maximal amplitude of the oscillations is ± 0.82 mm and ± 0.53 mm with standard deviation σ of 0.234 mm and 0.229 mm for x and y respectively. This will play a major role if we want to achieve alignment in the order of μm . On the other hand, the measured data do not have a large spread and they are oscillating around one point. Hence, it can be advantageous to extract information about the position by taking the mean of all centroid positions.

We decided to rebuild the experiment for a shorter distance in the laboratory to investigate, how well it is possible to extract the information about the position of a sensor relative to a reference position given by the beam.

Setup

The beam was propagated over 1.8 m on an optical table. SLB was projected straight on a camera chip without any objective lens. The SLB is stationary forming a reference, while the camera is moved by precise amounts using

the highly precise motorized stage hence representing an object of alignment. We used Thorlabs one-axis motorized stage MT1/M-Z8 with a resolution of 50 nm,

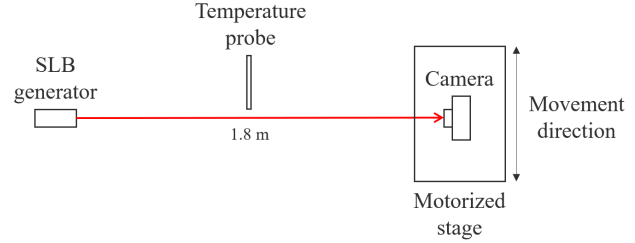


Figure 6: Schematic view of the setup.

The angles between the camera, motor, and laser were measured with a laser tracker. It was calculated that the perpendicularity misalignment between the camera chip, motor movement direction, and laser line is under $\pm 1^\circ$.

Results and discussion

The long-term stability of the line was measured for 11 hours (figure 7). We can see noticeable oscillations of the beam centroid with an amplitude of $\pm 5 \mu\text{m}$.

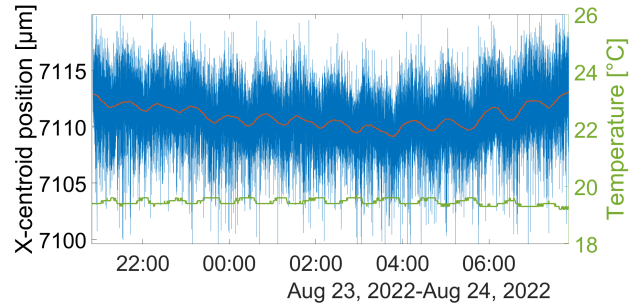


Figure 7: Stability of the beam was measured for 11 hours including the temperature measurement. The red line represents the moving average of the data for better visibility of the trend.

The temperature in the laboratory is relatively stable due to the air-conditioning (AC). It was measured with a resolution of 0.1 $^\circ\text{C}$. The temperature probe was placed approximately in the middle between the camera and the generator. The correlation between temperature and the position of the reference line is noticeable. As the temperature periodically changes, which is caused by the AC switching on and off, the same periodical change can be seen on the moving average of the centroid coordinate. The low-frequency change that is noticeable over the whole span of the data can be caused by the thermal expansion of the camera/generator holders, local temperature changes, or by a different, yet unknown factor.

The relative movement from the original position was also investigated. The motorized stage with the camera was moved for 15 μm . When it was in place the data acquisition

started for 20 seconds. We decided to use the GCoG algorithm to obtain the centroid position by analyzing 3 frames per second. The average standard deviation of the data in each position was $1.2 \mu\text{m}$. All values greater than 2σ were marked as noise and the rest of the data was averaged to obtain an average value of the position. This process was repeated several times.

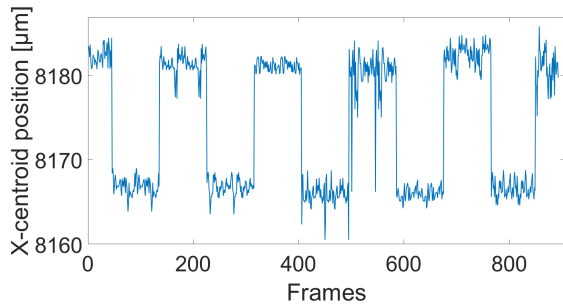


Figure 8: X-centroid coordinates obtained by GCoG while moving the camera for $15 \mu\text{m}$.

We were able to reconstruct the relative movement of $15 \mu\text{m}$ multiple times with an error of $\pm 1.3 \mu\text{m}$. The 1° misalignment of the setup means that the movement will not be completely perpendicular to the line, hence the systematic error is introduced. However, by simple trigonometric calculation, we can conclude, that this systematic error will be in the order of nm.

Results show that the refractive index oscillations of the propagation media caused by temperature instabilities, air fluctuations, and other variables represent a problem in future long-distance alignment applications as expected. We propose propagating the laser inside a tube, ideally under a vacuum, to obtain even better results.

CONCLUSION

Multiple algorithms for centroid coordinate detection of pseudo-non-diffractive beams, namely the BB and the SLB, were principally explained and compared. Results show that a preprocessing of the images is needed to obtain precise results. For the BFA, a circular mask to filter out the non-full ring of the beam needs to be used. The TCoG algorithm is very prone to the value of threshold level and background illumination changes. The GCoG has the best trade-off between speed, precision, and gamma parameter sensitivity for real measurements.

The potential of SLB for long-distance alignment applications was investigated. The bright central core can fit on the camera chip after propagating over 120 m hence it is possible to easily detect its centroid coordinates. However, it was confirmed that the atmospheric turbulence and surrounding conditions play a major role in the beam stability and detection of the magnitude of the misalignment. Refraction can also have a significant influence on the reference line's straightness.

The experiment was rebuilt for a shorter distance in the

laboratory. The beam was propagated in the free space and misalignment of $15 \mu\text{m}$ with an error of $\pm 1.3 \mu\text{m}$ over 2 m was detected multiple times. We propose propagating a beam inside a tube and vacuum in future experiments to minimize the effect of refractive index fluctuations.

ACKNOWLEDGEMENT

The authors acknowledge the financial support provided by the Knowledge Transfer group at CERN through the KT Fund.

This work has also been partly carried out within the framework of the project "Partnership for Excellence in Superprecise Optics" (Reg. No. CZ.02.1.01/0.0/0.0/16_026/008390) and co-funded by European Structural and Investment Funds.

REFERENCES

- [1] J.-C. Gayde and M. Sulc, "An Optical System for Producing a Structured Beam," EP3564734, 2019.
- [2] H. Mainaud Durand et. al., "HL-HLC Alignment Requirements and Associated Solutions," CERN, 2017, Copenhagen, Denmark, Proceedings of IPAC2017.
- [3] K. Polak, J.-C. Gayde, and M. Sulc, 'Structured laser beam for alignment and large-scale metrology', Euspens Conf., vol. EUSPEN2022, p. 4, 2022.
- [4] T. Suwada, M. Satoh, S. Telada, and K. Minoshima, 'Propagation and stability characteristics of a 500-m-long laser-based fiducial line for high-precision alignment of long-distance linear accelerators', Review of Scientific Instruments, vol. 84, no. 9, p. 093302, Sep. 2013, doi: 10.1063/1.4819960.
- [5] CERN. <https://home.cern/science/accelerators/compact-linear-collider>. Accessed 26. August 2021.
- [6] G. Stern, 'Study and development of a laser based alignment system for the compact linear collider', Doctoral Thesis, ETH Zurich, 2016. doi: 10.3929/ethz-a-010621412.
- [7] A. M. Nightingale and S. V. Gordeyev, 'Shack-Hartmann wavefront sensor image analysis: a comparison of centroiding methods and image-processing techniques', OE, vol. 52, no. 7, p. 071413, Mar. 2013, doi: 10.1117/1.OE.52.7.071413.